



Insights Into the Electronic Properties of PbBi Atomic Layers on Ge(111) and Si(111) Surfaces

A. N. Mihalyuk^{1,2*}, Y. E. Vekovshinin², L. V. Bondarenko², A. Y. Tupchaya², T. V. Utas², D. V. Gruznev², S. V. Ereemeev³, A. V. Zotov² and A. A. Saranin²

¹Institute of High Technologies and Advanced Materials, Far Eastern Federal University, Vladivostok, Russia, ²Institute of Automation and Control Processes FEB RAS, Vladivostok, Russia, ³Institute of Strength Physics and Materials Science SB RAS, Tomsk, Russia

Co-adsorption of Pb and Bi onto Si(111) and Ge(111) surfaces has been found to result in formation of atomic-layer PbBi compounds having similar structures. These are two co-existing crystalline PbBi phases with $2\sqrt{3} \times 2\sqrt{3}$ and 2×2 periodicities. Using density functional theory calculations, we found that these two phases present insulating and highly anisotropic metallic systems, respectively. However, electronic structure of the metallic 2×2 -PbBi phase on Ge(111) appears qualitatively different from that on the Si(111). We investigated electronic properties of the PbBi compound considering the effects induced by the different supporting substrates, namely Si(111) and Ge(111). As a part of comparative study, we made the chemical-bonding analysis and examined a free-standing PbBi layer inspecting the dependence of its spectral characteristics on the compressive/tensile strain. We believe that the present findings will play an important role in the development of new electronic devices fabricated in the ultimate two-dimensional limit.

Keywords: 2D materials, germanium, silicon, bismuth, lead

OPEN ACCESS

Edited by:

Ryan Requist,
Hebrew University of Jerusalem, Israel

Reviewed by:

Xiaotian Wang,
Southwest University, China
Chuanxu Ma,
University of Science and Technology
of China, China

*Correspondence:

A. N. Mihalyuk
mih-alexey@yandex.ru

Specialty section:

This article was submitted to
Quantum Materials,
a section of the journal
Frontiers in Materials

Received: 23 February 2022

Accepted: 13 April 2022

Published: 28 April 2022

Citation:

Mihalyuk AN, Vekovshinin YE,
Bondarenko LV, Tupchaya AY,
Utas TV, Gruznev DV, Ereemeev SV,
Zotov AV and Saranin AA (2022)
Insights Into the Electronic Properties
of PbBi Atomic Layers on Ge(111) and
Si(111) Surfaces.
Front. Mater. 9:882008.
doi: 10.3389/fmats.2022.882008

1 INTRODUCTION

Reducing crystalline materials from the bulk phase to the two dimensions (2D) creates a rich playground for different exotic electronic phases (Li et al., 2021). Discovery, characterization and control of electronic properties in the 2D materials is a central task of the surface science, where the quantum phenomena emerging in the ultimate two-dimensional case, when the thickness of the film is reduced down to the atomic-scale limit, are of especial interest.

Spin-orbit coupling (SOC) very often plays a key role in many electronic effects observed in the 2D materials. Among other heavy elements, lead and bismuth appear to be the very promising candidates for realizing exotic electronic states, since they have the largest atomic spin-orbit-coupling values and are known to realise unique quantum phenomena in a variety of perspective 1D and 2D materials, such as Pb atomic chains (Mihalyuk et al., 2020) and nanowires (Kopciuszynski et al., 2020) promising for realizing spin-polarized electron transport, plumbene (Zhao et al., 2016; Yuhara et al., 2019) and bismuthene (Luo and Xiang, 2015; Reis et al., 2017) are known to be topological materials, superconducting ultrathin Pb atomic films (Zhang et al., 2010) and ultrathin Bi films (Hirahara et al., 2011) demonstrating 1D topological spin-polarized edge states (Drozdov et al., 2014). There are various bismuth and lead compounds, which are found to be superconductors (Özer et al., 2007) or topological semimetals (Di Bernardo et al., 2021).

The substrate supporting 2D atomic layer plays a crucial role, since it shapes the geometry of the synthesized material and affects its electronic properties. The semiconductor materials became a

focus of substantial efforts to the surface engineering, especially silicon- and germanium-based systems (Pillarisetty, 2011). Recently it was found that PbBi compound of atomic thickness grown on silicon surface was found to demonstrate one-dimensional metallic spin-polarized electron states (Mihalyuk et al., 2021) a promising quantum effect relevant for spintronic applications. Remarkably that Pb-Bi films with a nominal thickness of about 4.8 nm grown on silicon demonstrate a superconducting transition at 6.13 K (Tian et al., 2021; Wang et al., 2022). In this regard there is an interest for engineering Pb and Bi containing materials on other semiconducting surfaces.

Among all of the known semiconductor materials, germanium has the highest hole mobility at room temperature (Sammak et al., 2019) (up to $10^6 \text{ cm}^2 (\text{Vs.})^{-1}$), which is about two times larger than the best group III–V *p*-type semiconductors and silicon. The high hole mobility in the germanium promotes the confinement of spins in the low-disorder Ge quantum dots by uniform potential landscapes (Hendrickx et al., 2018). Another milestone of Ge technology is that virtually every metal on Ge, including superconductors with high critical fields, demonstrate a Fermi level pinned close to the valence band (Dimoulas et al., 2006), which facilitates the injection of holes and, thus, the formation of ohmic superconductor/semiconductor contacts with low Schottky barrier, a key building block in hybrid quantum devices. These advantages make Ge a promising material for quantum technology, as it contains important parameters for semiconducting, superconducting, and topological quantum electronic devices (Scappucci et al., 2021); on the other hand, Ge emerges as an alternative for silicon replacement in future low-power logic applications (Swaminathan et al., 2010), and a key material for boosting the performance of nanodevices (Gomez et al., 2010).

Additional challenge for studying the PbBi layers on Ge(111) is associated with the recent theoretical predictions that Pb_3Bi compound with 1.0 ML of Pb and 0.33 ML of Bi possesses a number of fascinating properties, in particular the emergence of van Hove singularity and chiral topological superconducting state (Qin et al., 2019; Li et al., 2020; Sun et al., 2021). These attracting prospects have motivated us to probe the Ge(111) as a platform for synthesizing PbBi compound and studying emergent electronic states. In the present work, we have undertaken combined experimental and theoretical efforts to get insight into the properties of the new material, paying attention to the electronic band structure and impact of the supporting substrate through comparison of the properties of the parent PbBi/Ge(111) and PbBi/Si(111) systems.

2 EXPERIMENTAL AND COMPUTATIONAL DETAILS

Experiments were performed in the ultrahigh-vacuum Omicron MULTIPROBE system (base pressure $\leq 2.0 \times 10^{-10}$ Torr) by means of scanning tunneling microscopy (STM) and low-energy electron diffraction (LEED) methods. Ge(111) substrates were cleaned *in situ* by ion sputtering (0.6 keV for 20 min) followed by direct-current annealing at about 800°C. In order to achieve a well-ordered $c(8 \times 2)$

reconstruction, after three such cycles the samples were additionally annealed at 600°C for 3 min. Atomically-clean $\text{Si}(111)7 \times 7$ surfaces were prepared *in situ* by flashing to 1280°C after the samples were first outgassed at 600°C for several hours. Pb and Bi were deposited from the heated tantalum tubes and deposition rates were calibrated using STM observation of corresponding Pb and Bi reconstructions of Ge(111) surface. During the Pb deposition onto the Ge surface the sample temperature was held in the range from 100 to 200°C by indirect heating. In this temperature range, the temperature was measured by a K-type thermocouple installed into the sample stage. STM images were acquired using Omicron variable-temperature STM-XA operating in a constant-current mode. Mechanically cut PtIr tips were used as STM probes after annealing in vacuum.

Density functional theory (DFT) calculations were performed using Vienna Ab initio Simulation Package (VASP) (Kresse and Hafner, 1993; Kresse and Furthmüller, 1996), with core electrons represented by projector augmented wave (PAW) potentials (Blöchl, 1994). The generalized gradient approximation of Perdew, Burke, and Ernzerhof (GGA-PBE) (Perdew et al., 1996) to the exchange-correlation functional was employed for structure relaxation. To simulate the PbBi structure on Ge(111) surface we used a slab consisting of 5 bi-layers (BL) of the substrate with the PBE-optimized bulk Ge lattice constant. Hydrogen atoms were used to passivate the Ge dangling bonds at the bottom of the slab. The atomic positions of PbBi atoms and atoms of Ge layers within the two topmost BLs of the slab were optimized. The geometry optimization was performed until the residual forces on atoms became smaller than $10 \text{ meV}/\text{Å}$. The $7 \times 7 \times 1$ and $5 \times 5 \times 1$ *k*-point mesh was used to sample the $(\text{Pb,Bi})/\text{Ge}(111)-2 \times 2$ and $(\text{Pb,Bi})/\text{Ge}(111)2\sqrt{3} \times 2\sqrt{3}$ surface Brillouin zones, respectively. For getting an accurate Ge band gap we applied the DFT-*U* Hubbard correction method (Anisimov et al., 1991; Dudarev et al., 1998). The scalar relativistic effects and the spin-orbit coupling were taken into account for calculating the band structures. In order to find the most stable PbBi structures on Ge(111) surface we used the *ab initio* random structure searching (AIRSS) approach (Pickard and Needs, 2011). In all calculations were used Pb and Bi pseudo-potentials containing *d*-electrons.

For more detailed analysis of the interactions of the Pb and Bi atoms with Ge/Si substrates and each other, we performed projected crystal orbital Hamilton population (pCOHP) analysis, (Dronskowski and Bloechl, 1993; Deringer et al., 2011), which is a partitioning scheme of the Kohn–Sham band structure energy in the plane-wave DFT calculations in terms of orbital-pair contributions. For this, we used the Local-Orbital Basis Suite Towards Electronic-Structure Reconstruction (LOBSTER) code (Maintz et al., 2016). The bond-analytical pCOHP provides quantitative information on the bonding, nonbonding, and antibonding contributions in the plane-wave DFT calculations.

3 RESULTS AND DISCUSSION

3.1 Samples Preparation and Atomic Structure

In the present STM and LEED experiments, we explored co-adsorption of Pb and Bi onto the Ge(111) and Si(111) surfaces in

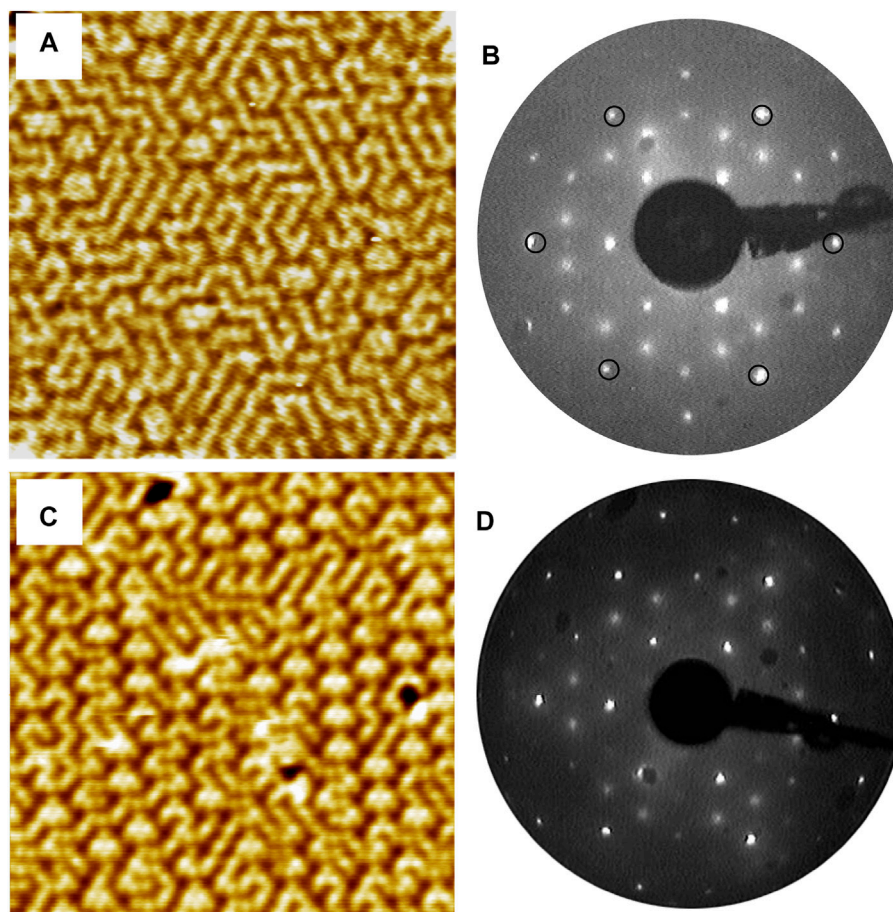
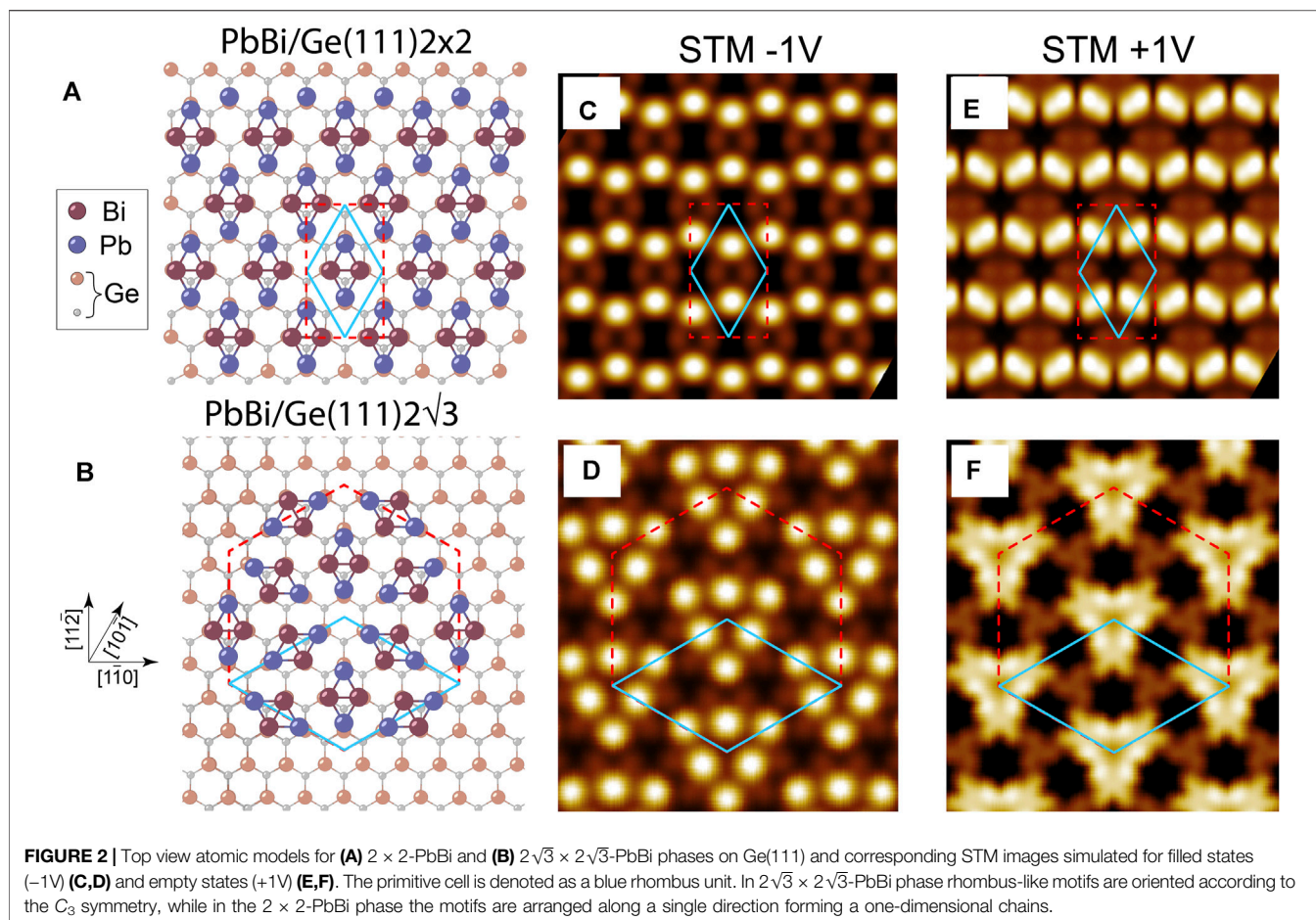


FIGURE 1 | Morphology and arrangement of the PbBi atomic layer adsorbed on different substrates. The Ge(111)-based system is characterised by **(A)** $25 \times 29 \text{ nm}^2$ (-1.5 V , 0.9 nA) STM image; **(B)** 79 eV LEED pattern. The Si(111)-based system is characterised by **(C)** $15 \times 15 \text{ nm}^2$ (-0.002 V , 200 pA) STM image; **(D)** 54 eV LEED pattern, recorded at 78 K

a wide range of adsorbate coverages, namely in the Ge(111) case we varied the concentration of Bi adsorption onto the β - $\sqrt{3}$ -Pb-Ge(111) substrate from 0.1 to 0.8 ML (see **Supplementary Figure S1**). In the most cases, the resultant PbBi layers display heterogeneous structures, where patches of the PbBi compounds are surrounded by patches of the bare Pb and Bi reconstructions or disordered surface regions (**Supplementary Figure S1**). The only well-defined PbBi compounds formed in the both systems contain 0.5 ML of Bi [monolayer, $7.2 \cdot 10^{14} \text{ cm}^{-2}$ and $7.8 \cdot 10^{14} \text{ cm}^{-2}$ for Ge(111) and Si(111), respectively] and the same concentration of Pb (see high-resolution STM images in **Figures 1A,C**, respectively). These compounds have two distinct phases, the 2×2 -PbBi and $2\sqrt{3} \times 2\sqrt{3}$ -PbBi (hereinafter referred to as 2×2 and $2\sqrt{3}$, respectively) as follows from the LEED patterns (**Figures 1B,D**). The attempt to fabricate recently predicted $\text{Pb}_3\text{Bi}-\sqrt{3}$ -Ge(111) phase (Qin et al., 2019; Li et al., 2020; Sun et al., 2021) through simultaneous adsorption of 1.00 ML Pb and 0.33 ML Bi onto the Ge(111) substrate resulted to the formation of β - $\sqrt{3}$ -Pb phase along with patches of the mixture of $2\sqrt{3}$ and 2×2 -PbBi phases containing mass transfer islands (see **Supplementary Figure S2**).

Among other varied parameters of Pb and Bi co-adsorption onto the Ge(111) and Si(111) surfaces, there were the growth temperature, typically between room-temperature (RT) and 350°C , and the order of the adsorbed elements, i.e., the PbBi phases can be built either by simultaneous deposition of Pb and Bi elements (followed by annealing) or using successive depositions with intermediate annealing after the deposition of the first adsorbate. General behavior of the PbBi/Ge(111) and PbBi/Si(111) systems was found to be very similar.

Based on experimental data (the surface concentration of each element and periodicity parameters) we conducted the comprehensive *ab initio* total-energy calculations to find the ground-state atomic models for the both phases, applying AIRSS method. The top views of the obtained lowest-energy models are displayed in **Figures 2A,B**, where one can see the presence of the distinct rhombus-like motif serving as a building block in both phases. The motif includes pair of Bi atoms and pair of Pb atoms, which all are located in the vicinities of the on-top (T1) sites on the bulk-truncated Ge(111) surface. In the rhombus, Bi dimer forms a short diagonal, while the two separated Pb atoms form a long rhombus diagonal, each being bonded to the



bismuth atoms. One can see that in the 2×2 -PbBi phase motifs are oriented in a single direction (Figure 2A), while in the $2\sqrt{3}$ -PbBi phase motifs are arranged according to the C_3 symmetry (Figure 2B), consequently their unit cells contain one and three rhombi, respectively. According to the total-energy calculations the 2×2 -PbBi atomic model is more stable than the $2\sqrt{3}$ -PbBi model by 10 meV per 1×1 unit cell. This relatively small energy difference accounts for the simultaneous growth of the two crystalline phases on Ge(111) surface with slight energetic favor for the 2×2 phase.

Simulated STM images of the 2×2 -PbBi phase at the negative bias (or filled states) show the general honeycomb-like appearance (Figure 2C) (as it was also observed in experimental measurements (Figure 1A), although the detailed consideration reveals the 1D nature of STM pattern where bright protrusions are associated with Pb atoms forming a zig-zag charge chain. The positive bias (or empty states) STM simulation produces the very similar one-dimensional appearance of the pattern with bright protrusions associated with Pb-Pb bonds. The STM simulation of the $2\sqrt{3}$ -PbBi phase (Figure 2E) at the negative bias gives a bright triangular appearance, while at the positive bias one may see the network-like structure with the big bright three-fold patterns connected by the small faint triangles around (Figure 2F).

It is worth noting that established PbBi-Ge(111) ground-state atomic models for two coexisting phases are akin to the recently discovered PbBi-Si(111) phases (Mihalyuk et al., 2021). For this reason, below we give a detailed comparison between the electronic structures of the 2×2 -PbBi and $2\sqrt{3}$ -PbBi phases on the Ge(111) with their counterparts on the silicon substrate.

3.2 Electronic Properties

Before we start the inspection of electronic properties of the considered systems, let us address the lattice symmetry issue, since it is indispensable for the proper understanding of the emerging electronic effects. The underlying Ge(111) substrate has a C_{3v} symmetry (plane-group $p3m$), while the rhombus-like motif has a C_{1h} symmetry (plane-group $p1$), arising from a particular arrangement of the constituent Pb and Bi atoms. So the presence of the PbBi rhombus on the Ge(111) substrate reduces the total symmetry of the system down to C_{1h} for the 2×2 case since it contains only one rhombus element bringing the structural anisotropy, but this does not happen in the case of the $2\sqrt{3}$ -phase where all three rhombi are arranged in a C_{3v} symmetry manner (as shown in Figure 2B), and, thus, preserving the total C_{3v} symmetry of the structure.

Let us start our consideration with the electronic band structure of (Pb,Bi)/Ge(111)- $2\sqrt{3}$ phase. Figure 3A shows the

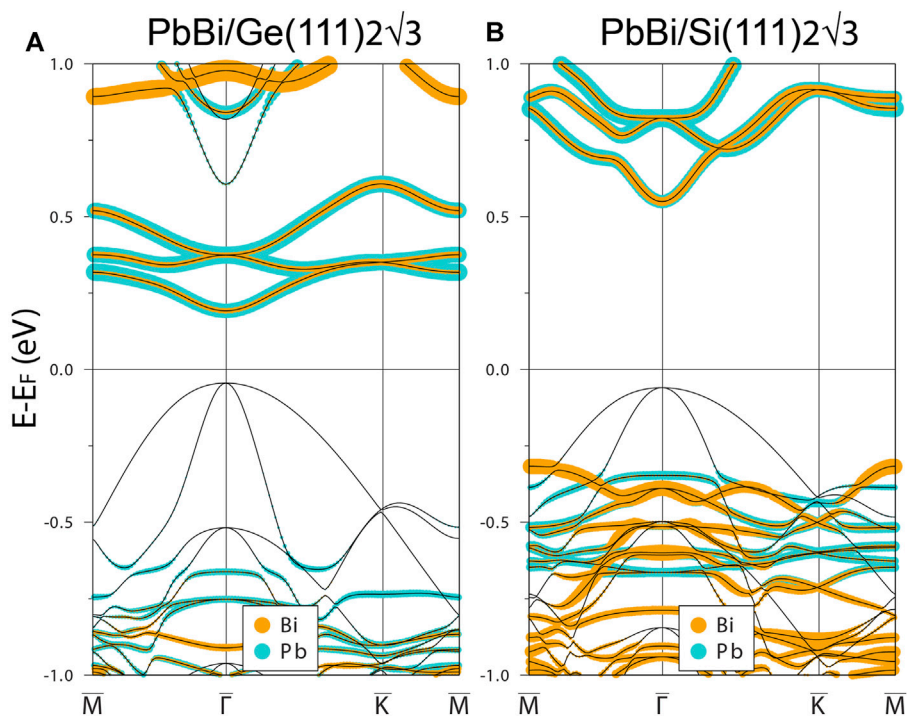


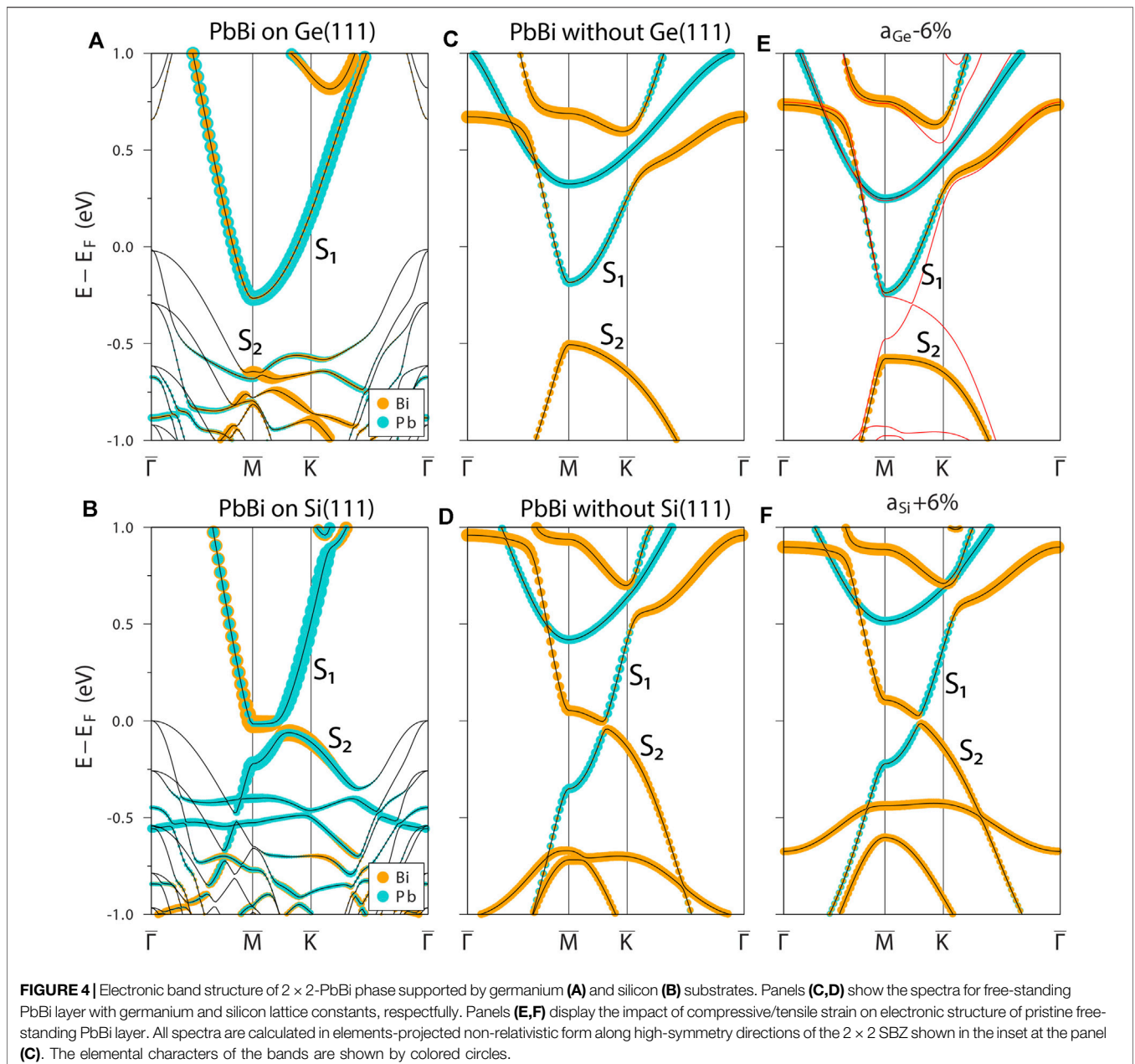
FIGURE 3 | The electronic band structure of $2\sqrt{3}$ -PbBi phase adsorbed on **(A)** germanium, and **(B)** silicon substrates. Both figures present elements-projected non-relativistic spectra, where the elemental characters of the bands are shown by colored circles, blue and orange for Pb and Bi orbitals, respectively.

non-relativistic spectrum where the projections of Pb and Bi orbitals are shown by blue and orange circles, respectively. The spectrum has an insulating character with a bunch of the weakly-dispersive unoccupied surface bands propagating in the germanium band gap within the [0.2; 0.6] eV energy range above E_F . These bands are characterized by the contributions of both Pb and Bi orbitals. As expected the electronic dispersion of the spectrum has a clear isotropic character typical for the C_{3v} symmetry systems. Insulating character of the band structure is retained even after including SOC effect into band structure calculation, which will be discussed below.

One can trace the electronic character of the system from the structural considerations. Note that the geometry itself of the $2\sqrt{3}$ -PbBi atomic model induces its insulating nature since all Pb atoms (accumulating the charges, as seen in the STM images in **Figure 2D**) in the unit cell are ordered as isolated clusters separated by non-metallic bismuth atoms around (see **Figure 2D**); as a result the weakly dispersive bands and zero density of states at the Fermi level are expected in the system.

Interesting that the $2\sqrt{3}$ -PbBi compound grown on Si(111) surface, which atomic model is almost the same, has the qualitatively very similar dispersion character (**Figure 3B**) with no metallic bands and large gap around Fermi level. The higher position of the in-gap PbBi bands on Si(111) in contrast to Ge(111) is due to the fact that Si bulk gap almost two times larger than the Ge bulk gap. The discussed spectrum is calculated according to the corresponding model from Ref (Mihalyuk et al., 2021).

Now let us move to the (Pb,Bi)/Ge(111)- 2×2 phase, which electronic spectrum is presented in **Figure 4A** along with analogous dispersions calculated for Si(111)-based system (**Figure 4B**); such a comparison allows us to trace the role of the supporting substrate on the resultant electronic properties. From the element-projected non-relativistic spectrum shown in **Figure 4A** one can see the highly dispersing S1 metallic surface band propagating within the germanium bulk gap and mainly filled by Pb states denoted in spectrum by blue colored circles. Intersection of the Fermi level gives rise to electron pocket around the \bar{M} point. Another Bi-induced electronic band S2 (marked by orange circles) strongly hybridizes with the germanium bulk states and completely merged in the valence band area. Remarkably, the analogous spectrum for the Si-supported system **Figure 4B** qualitatively has a very different character showing the hybridization of S1 and S2 surface bands with each other resulting in appearance of 70 meV gap below the Fermi level in the middle of the \bar{M} - \bar{K} direction. The difference between spectra of silicon- and germanium-based structures is a bit unexpected, since their atomic models have almost identical adsorption geometry. In order to exclude the hybridization effects caused by the substrates we removed them from the structural model and calculated the spectra for 2×2 -PbBi free-standing layers keeping their internal structure and lattice constants defined by the corresponding Ge(111)- or Si(111)- 2×2 substrate (**Figures 4C,D**, respectively). One can see that the dispersion character of S1 and S2 bands qualitatively is the same either Ge or Si substrates support the PbBi layer, or



not. One may conclude that substrates do not affect the character of the electronic spectra significantly, but rather it seems that the lattice constant of the system is a main issue. As known, the Ge(111) lattice constant $a_{\text{Ge}} = 4.09 \text{ \AA}$ is by $\approx 6\%$ larger than the silicon constant $a_{\text{Si}} = 3.86 \text{ \AA}$, therefore we decide to apply a 6% compressive/tensile strain to Ge/Si-derived free-standing atomic models to bring their lattice constants into line with the parameters of opposite model in order to see if the dispersions will be qualitatively changed under that factor. **Figures 4E,F** show the results of the strain test on electronic structure; from here one may see almost no changes in the character of the electronic structure, which is again a bit unexpected.

The last point that remains to be explored is the geometry of the rhombus itself, which is apparently expected to determine the principal features of the electronic spectrum. **Figure 5** give the comprehensive comparison between silicon- and germanium-based models of the 2×2 phase. It is worth to note that PbBi rhombi on both substrates are not equilateral and have the buckling geometry, i.e., the heights of Pb_1 and Pb_2 atoms with respect to the position of Bi atoms are slightly different due to the different relief of the underlying substrates. In spite of $\approx 6\%$ difference between Ge(111) and Si(111) surface unit cell parameters one may see that rhombus parameters such as Bi-Bi, Pb-Bi bondlengths and inside obtuse angle denoted as α are changed insignificantly, while Pb-Pb bondlength and angle of the

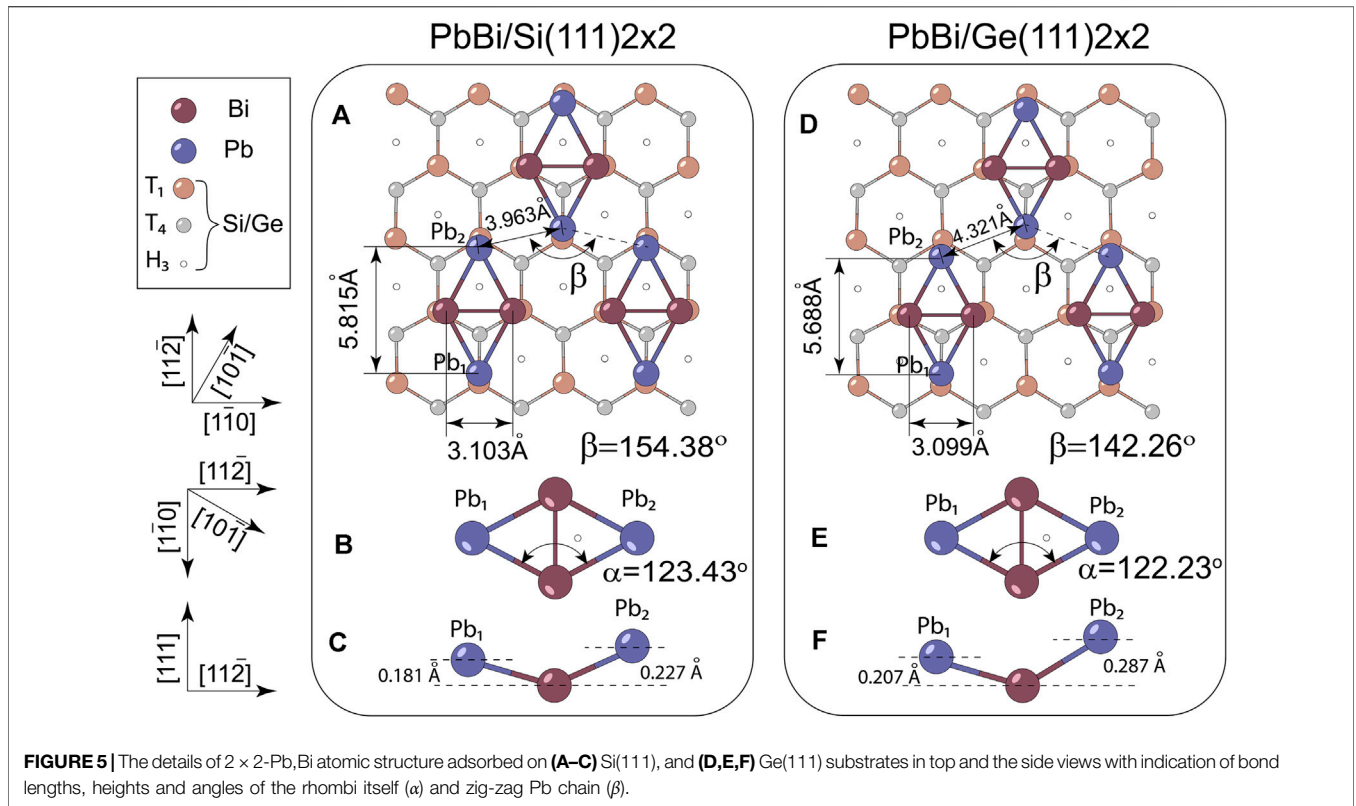


TABLE 1 | Bond energies, E (eV), as obtained from integrated pCOHP and corresponding bond lengths, d (Å), between neighboring atoms in the 2×2 phases on Si(111) and Ge(111).

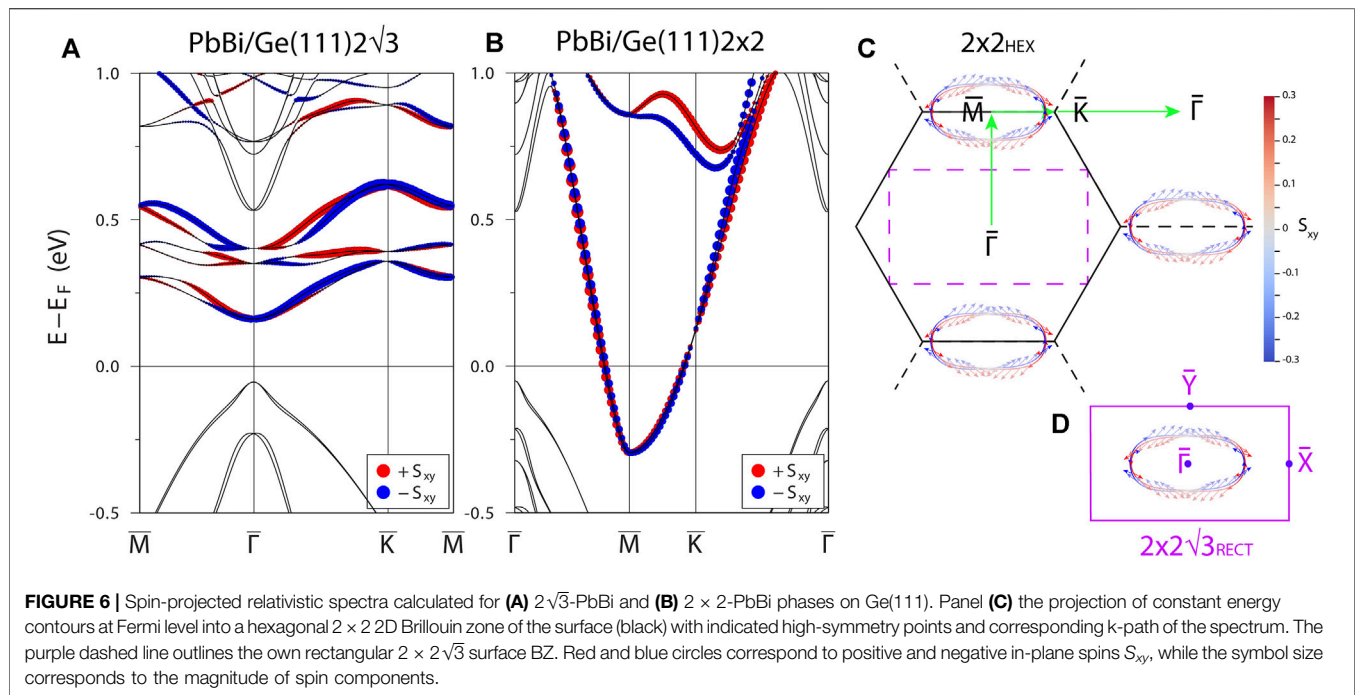
(Pb,Bi)/Si(111)- 2×2			(Pb,Bi)/Ge(111)- 2×2		
bond	E	d	bond	E	d
Pb ₁ -Si	3.214	2.793	Pb ₁ -Ge	3.125	2.854
Pb ₂ -Si	3.231	2.791	Pb ₂ -Ge	3.099	2.861
Bi-Si	3.601	2.711	Bi-Ge	3.414	2.780
Bi-Bi	2.123	3.103	Bi-Bi	2.035	3.099
Pb ₁ -Bi	1.833	3.284	Pb ₁ -Bi	1.913	3.245
Pb ₂ -Bi	1.731	3.320	Pb ₂ -Bi	1.902	3.251
Pb ₁ -Pb ₂	0.490	3.963	Pb ₁ -Pb ₂	0.243	4.321

zig-zag Pb chain denoted as β are changed crucially and, thus, deserve special consideration.

In order to scrutinize the bond strengths within rhombi and between rhombi and Ge (Si) substrates, we conducted a chemical-bonding analysis using Crystal Orbital Hamilton Populations method, which results are summarised in **Table 1**. One can see that among various bonds in the system the strongest are those between Pb (Bi) atoms and nearest substrate atoms, wherein the strength of Pb-Si and Bi-Si interactions is a bit larger than Pb-Ge and Bi-Ge interactions, which is consistent with the shorter bond lengths in the Si case, and longer in the Ge case. However, as we showed above in **Figure 4**, the interaction of the PbBi atomic layer with underlying substrate does not qualitatively affect the dispersion of the PbBi bands near the Fermi level. Within the

distorted rhombus, the Bi-Bi bond is a bit weaker in the Ge-supported structure, whereas the bonds between Bi atoms and two differently located Pb atoms are stronger in this structure in comparison with the Si case. The weakest bond in the PbBi atomic layer is the Pb-Pb one and its length defines the proximity of neighboring rhombi or density of motifs packing. Remarkably, among all other bonds that one has almost the double difference in energy values between Ge and Si cases (see **Table 1**).

With motivation to estimate the impact of Pb-Pb interaction on principal characteristics of electronic spectrum of free-standing PbBi layer we applied a 6% compressive strain to the lattice vectors of Ge-derived unit cell but keeping all parameters of PbBi rhombus unchanged (unlike to the previous strain test, where the uniform changing of all rhombus parameters also took the place). In the result the Pb-Pb distances and angle in the Pb-Pb “zig-zag chain” became almost the same ($d_{\text{Pb-Pb}} = 3.993$ Å and $\beta = 150.73^\circ$) as in the Si-derived cell. This structural transformation dramatically changed the electronic spectrum (see the red dispersion curves in **Figure 4E**) shaping it to the character very similar to the Si-derived case (**Figure 4D**). However, under the uniform 6% compression the Pb-Pb bond length is almost the same, $d_{\text{Pb-Pb}} = 4.084$ Å like in the former structure, while the β angle is equal to that the undeformed structure, 142.26° . Thus, one can conclude that change in the β angle of the Pb-Pb zig-zag chain is a key factor responsible for a significant decrease in hybridization between the rhombi (decrease in the Pb-Pb bond strength) and, as a result, an increase in hybridization within PbBi rhombi leading to the modification of the electronic band structure near the Fermi level.



Let us finally examine the impact of spin-orbit coupling effect on the electronic properties of $2\sqrt{3}$ -PbBi and 2×2 -PbBi phases. **Figures 6A,B** display relativistic spin-projected spectra for both phases, from which one can see that dispersion character did not change substantially in comparison with non-relativistic spectra shown in **Figure 3A** and **Figure 4A**. The spectrum of $2\sqrt{3}$ -PbBi (**Figure 6A**) demonstrates relatively small band splitting over the entire k space; the bands have isotropic character with helical behaviour of spin components typical for the system with C_{3v} symmetry. The electronic band structure of 2×2 -PbBi phase **Figure 6B** in the presence of SOC shows only tiny spin splitting in contrast to the related Si-based phase where spin-splitting is huge (Mihalyuk et al., 2021). The geometry of 2×2 -PbBi atomic model as noticed above is characterized by a C_{1h} symmetry and that, as seen in the Fermi contours in **Figure 6C**, it shapes the electronic band structure as a quasi-one-dimensional metallic system with highly anisotropic constant energy contours (elongated along each third \bar{K} - \bar{M} - \bar{K} side of the hexagonal 2×2 Brillouin zone (**Figure 6C**). The 1D character of 2×2 -PbBi electronic structure may be unambiguously confirmed by calculating the spectrum within rectangular $2 \times 2\sqrt{3}$ unit-cell, which takes into account the C_{1h} character of the model. Due to the Brillouin zone folding the spin-split bands, dispersing along the \bar{K} - \bar{M} - \bar{K} direction of hexagonal 2×2 BZ (**Figure 6C**), appear in the \bar{X} - $\bar{\Gamma}$ - \bar{X} direction of the own rectangular $2 \times 2\sqrt{3}$ surface BZ as shown in **Figure 6D**.

4 CONCLUSION

We have successfully grown and investigated the structural and electronic characteristics of PbBi atomic layers on Ge(111) and Si(111) surfaces. According to the STM and LEED observations,

simultaneous formation of the two crystalline phases with the $2\sqrt{3} \times 2\sqrt{3}$ and 2×2 periodicities takes place. Comprehensive DFT calculations revealed the ground-state atomic models for the both phases, where a rhombus-like motif serves a key building block in both models. Despite the structure of the PbBi 2D compounds grown on germanium surface is similar to that on the silicon substrate investigated recently, the electronic spectra of the Ge-supported phases have differences. The $2\sqrt{3}$ -PbBi phase on Ge(111) has an insulating character with a sizable gap around Fermi level, which is qualitatively similar to the Si(111)-based counterpart. However, due to the smaller bulk gap in the germanium, the adlayer bands lie closer to the valence band, comparing with the former case. At the same time, the spin splitting of these bands is just as insignificant as in the $2\sqrt{3}$ -PbBi phase on Si(111). Another coexisting 2×2 -PbBi phase on Ge(111) has a pronounced anisotropy of the band structure stemming from the C_{1h} geometry of its atomic model and is characterized as a metallic quasi-one-dimensional system. This feature is also much similar to the silicon-supported phase, but qualitatively there is a great difference in the character of hybridization of the Pb- and Bi-derived bands between Ge- and Si-based systems. The chemical-bonding analysis of the PbBi 2×2 phases on Ge(111) and Si(111) revealed that among others the Pb-Pb bond energies differ most significantly, which are two times less on germanium than on silicon. The compressive/tensile-strain tests probed to the free-standing atomic models revealed that change in the angle of the Pb-Pb zig-zag chain has a greater impact on the electronic spectrum rather than the Pb-Pb bond length as well as a uniform deformation of the rhombi themselves. Another important difference between electronic structure of the Si- and Ge-supported 2×2 phase is a magnitude of the spin

splitting. The SOC-induced spin splitting is only tiny in the latter case while it is huge in the Si-supported phase that results in appearance of spin-polarized electronic state near the Fermi level. These insights into the interplay of geometry and electron correlations in (Pb,Bi)/Ge(111)-2 × 2 atomic layer can open the opportunities for designing advanced phases for future nanoelectronic devices with tunable electronic properties.

DATA AVAILABILITY STATEMENT

The raw data supporting the conclusion of this article will be made available by the authors, without undue reservation.

AUTHOR CONTRIBUTIONS

AM and SE wrote the manuscript and performed the theoretical calculation and analysis, AM and TU produced the figures, LB did the fabrication of materials, AT performed the material characterization, TU analyzed the data, YV performed STM measurements under the guidance of DG, SE contributed to the developing of main concept of the study,

AZ contributed to the review and editing of the paper, AS supervised the work and contributed with constructive discussions. All authors discussed the results and implications and commented extensively on the manuscript at all stages.

FUNDING

The experimental work and calculations of germanium-based systems were supported by the RSF Grant No. 21-72-00127. The calculations of silicon-based systems were supported by the Government research assignment for ISPMS SB RAS, project FWRW-2022-0001. The calculations were conducted using the equipment of Shared Resource Center “Far Eastern Computing Resource” IACP FEB RAS (<https://cc.dvo.ru>).

SUPPLEMENTARY MATERIAL

The Supplementary Material for this article can be found online at: <https://www.frontiersin.org/articles/10.3389/fmats.2022.882008/full#supplementary-material>

REFERENCES

- Anisimov, V. I., Zaanen, J., and Andersen, O. K. (1991). Band Theory and Mott Insulators: Hubbard U Instead of Stoner I. *Phys. Rev. B* 44, 943–954. doi:10.1103/physrevb.44.943
- Blöchl, P. E. (1994). Projector Augmented-Wave Method. *Phys. Rev. B* 50, 17953–17979. doi:10.1103/physrevb.50.17953
- Deringer, V. L., Tchougréeff, A. L., and Dronskowski, R. (2011). Crystal Orbital Hamilton Population (COHP) Analysis as Projected from Plane-Wave Basis Sets. *J. Phys. Chem. A* 115, 5461–5466. doi:10.1021/jp202489s
- Di Bernardo, I., Hellerstedt, J., Liu, C., Akhgar, G., Wu, W., Yang, S. A., et al. (2021). Progress in Epitaxial Thin-Film Na₃Bi as a Topological Electronic Material. *Adv. Mat.* 33, 2005897. doi:10.1002/adma.202005897
- Dimoulas, A., Tsipas, P., Sotiropoulos, A., and Evangelou, E. K. (2006). Fermi-level Pinning and Charge Neutrality Level in Germanium. *Appl. Phys. Lett.* 89, 252110. doi:10.1063/1.2410241
- Dronskowski, R., and Blochl, P. E. (1993). Crystal Orbital Hamilton Populations (COHP): Energy-Resolved Visualization of Chemical Bonding in Solids Based on Density-Functional Calculations. *J. Phys. Chem.* 97, 8617–8624. doi:10.1021/j100135a014
- Drozdz, I. K., Alexandradinata, A., Jeon, S., Nadj-Perge, S., Ji, H., Cava, R. J., et al. (2014). One-dimensional Topological Edge States of Bismuth Bilayers. *Nat. Phys.* 10, 664–669. doi:10.1038/nphys3048
- Dudarev, S. L., Botton, G. A., Savrasov, S. Y., Humphreys, C. J., and Sutton, A. P. (1998). Electron-energy-loss Spectra and the Structural Stability of Nickel Oxide: An LSDA+U Study. *Phys. Rev. B* 57, 1505–1509. doi:10.1103/physrevb.57.1505
- Gomez, L., Ni Chlairigh, C., Hashemi, P., and Hoyt, J. L. (2010). Enhanced Hole Mobility in High Ge Content Asymmetrically Strained-SiGe P-MOSFETs. *IEEE Electron Device Lett.* 31, 782–784. doi:10.1109/led.2010.2050574
- Hendrickx, N. W., Franke, D. P., Sammak, A., Kouwenhoven, M., Sabbagh, D., Yeoh, L., et al. (2018). Gate-controlled Quantum Dots and Superconductivity in Planar Germanium. *Nat. Commun.* 9, 2835. doi:10.1038/s41467-018-05299-x
- Hirahara, T., Bihlmayer, G., Sakamoto, Y., Yamada, M., Miyazaki, H., Kimura, S.-i., et al. (2011). Interfacing 2D and 3D Topological Insulators: Bi(111) Bilayer on Bi₂Te₃. *Phys. Rev. Lett.* 107, 166801. doi:10.1103/PhysRevLett.107.166801
- Kopciuszynski, M., Stepniak-Dybala, A., Dachniewicz, M., Żurawek, L., Krawiec, M., and Zdyb, R. (2020). Hut-shaped Lead Nanowires with One-Dimensional Electronic Properties. *Phys. Rev. B* 102, 125415. doi:10.1103/PhysRevB.102.125415
- Kresse, G., and Furthmüller, J. (1996). Efficient Iterative Schemes For Ab Initio Total-Energy Calculations Using a Plane-Wave Basis Set. *Phys. Rev. B* 54, 11169–11186. doi:10.1103/physrevb.54.11169
- Kresse, G., and Hafner, J. (1993). Ab Initio Molecular Dynamics for Liquid Metals. *Phys. Rev. B* 47, 558–561. doi:10.1103/physrevb.47.558
- Li, L., Ren, S., Qin, W., Zhang, S., Wan, X., Jia, Y., et al. (2020). Emergence of Van Hove Singularity and Topological States in Pb₃Bi/Ge(111) Rashba Systems. *Phys. Rev. B* 102, 035150. doi:10.1103/PhysRevB.102.035150
- Li, W., Qian, X., and Li, J. (2021). Phase Transitions in 2D Materials. *Nat. Rev. Mater.* 6, 829–846. doi:10.1038/s41578-021-00304-0
- Luo, W., and Xiang, H. (2015). Room Temperature Quantum Spin Hall Insulators with a Buckled Square Lattice. *Nano Lett.* 15, 3230–3235. doi:10.1021/acs.nanolett.5b00418
- Maintz, S., Deringer, V. L., Tchougréeff, A. L., and Dronskowski, R. (2016). LOBSTER: A Tool to Extract Chemical Bonding from Plane-Wave Based DFT. *J. Comput. Chem.* 37, 1030–1035. doi:10.1002/jcc.24300
- Mihalyuk, A. N., Bondarenko, L. V., Tupchaya, A. Y., Utas, T. V., Vekovshinin, Y. E., Gruznev, D. V., et al. (2021). One-dimensional Spin-Polarized Electron Channel in the Two-Dimensional PbBi Compound on Silicon. *Phys. Rev. B* 104, 125413. doi:10.1103/PhysRevB.104.125413
- Mihalyuk, A. N., Chou, J. P., Ereemeev, S. V., Zotov, A. V., and Saranin, A. A. (2020). One-dimensional Rashba States in Pb Atomic Chains on a Semiconductor Surface. *Phys. Rev. B* 102, 035442. doi:10.1103/PhysRevB.102.035442
- Özer, M. M., Jia, Y., Zhang, Z., Thompson, J. R., and Weitering, H. H. (2007). Tuning the Quantum Stability and Superconductivity of Ultrathin Metal Alloys. *Science* 316, 1594–1597. doi:10.1126/science.1142159
- Perdew, J. P., Burke, K., and Ernzerhof, M. (1996). Generalized Gradient Approximation Made Simple. *Phys. Rev. Lett.* 77, 3865–3868. doi:10.1103/PhysRevLett.77.3865
- Pickard, C. J., and Needs, R. J. (2011). Ab Initio Random Structure Searching. *J. Phys. Condens. Matter* 23, 053201. doi:10.1088/0953-8984/23/5/053201
- Pillarisetty, R. (2011). Academic and Industry Research Progress in Germanium Nanodevices. *Nature* 479, 324–328. doi:10.1038/nature10678

- Qin, W., Li, L., and Zhang, Z. (2019). Chiral Topological Superconductivity Arising from the Interplay of Geometric Phase and Electron Correlation. *Nat. Phys.* 15, 796–802. doi:10.1038/s41567-019-0517-5
- Reis, F., Li, G., Dudy, L., Bauernfeind, M., Glass, S., Hanke, W., et al. (2017). Bismuthene on a SiC Substrate: A Candidate for a High-Temperature Quantum Spin Hall Material. *Science* 357, 287–290. doi:10.1126/science.aai8142
- Sammak, A., Sabbagh, D., Hendrickx, N. W., Lodari, M., Paquelet Wuetz, B., Tosato, A., et al. (2019). Shallow and Undoped Germanium Quantum Wells: A Playground for Spin and Hybrid Quantum Technology. *Adv. Funct. Mat.* 29, 1807613. doi:10.1002/adfm.201807613
- Scappucci, G., Kloeffer, C., Zwanenburg, F. A., Loss, D., Myronov, M., Zhang, J.-J., et al. (2021). The Germanium Quantum Information Route. *Nat. Rev. Mater* 6, 926–943. doi:10.1038/s41578-020-00262-z
- Sun, S., Qin, W., Li, L., and Zhang, Z. (2021). Chiral Topological Superconducting State with Chern Number $C = -2$ in pb3Bi/Ge(111). *Phys. Rev. B* 103, 235149. doi:10.1103/PhysRevB.103.235149
- Swaminathan, S., Shandalov, M., Oshima, Y., and McIntyre, P. C. (2010). Bilayer Metal Oxide Gate Insulators for Scaled Ge-Channel Metal-Oxide-Semiconductor Devices. *Appl. Phys. Lett.* 96, 082904. doi:10.1063/1.3313946
- Tian, M.-Y., Wang, J.-F., Du, H.-J., Ma, C.-X., and Wang, B. (2021). Characterization of Structure and Superconducting Properties of Low-Temperature Phase of Pb-Bi Alloy Films. *Acta Phys. Sin.* 70, 170703. doi:10.7498/aps.70.20210482
- Wang, J. F., Tian, M. Y., Du, H. J., Ma, C. X., and Wang, B. (2022). Structural and Superconducting Properties of Ultrathin Pbbi₃ Films Fabricated at Low Temperature. *Acta Phys. Sin.* doi:10.7498/aps.71.20220050
- Yuhara, J., He, B., Matsunami, N., Nakatake, M., and Le Lay, G. (2019). Graphene's Latest Cousin: Plumbene Epitaxial Growth on a "Nano WaterCube". *Adv. Mat.* 31, 1901017. doi:10.1002/adma.201901017
- Zhang, T., Cheng, P., Li, W.-J., Sun, Y.-J., Wang, G., Zhu, X.-G., et al. (2010). Superconductivity in One-Atomic-Layer Metal Films Grown on Si(111). *Nat. Phys.* 6, 104–108. doi:10.1038/nphys1499
- Zhao, H., Zhang, C.-w., Ji, W.-x., Zhang, R.-w., Li, S.-s., Yan, S.-s., et al. (2016). Unexpected Giant-Gap Quantum Spin Hall Insulator in Chemically Decorated Plumbene Monolayer. *Sci. Rep.* 6, 20152. doi:10.1038/srep20152

Conflict of Interest: The authors declare that the research was conducted in the absence of any commercial or financial relationships that could be construed as a potential conflict of interest.

Publisher's Note: All claims expressed in this article are solely those of the authors and do not necessarily represent those of their affiliated organizations, or those of the publisher, the editors and the reviewers. Any product that may be evaluated in this article, or claim that may be made by its manufacturer, is not guaranteed or endorsed by the publisher.

Copyright © 2022 Mihalyuk, Vekovshinin, Bondarenko, Tupchaya, Utas, Gruznev, Eremeev, Zotov and Saranin. This is an open-access article distributed under the terms of the Creative Commons Attribution License (CC BY). The use, distribution or reproduction in other forums is permitted, provided the original author(s) and the copyright owner(s) are credited and that the original publication in this journal is cited, in accordance with accepted academic practice. No use, distribution or reproduction is permitted which does not comply with these terms.